CHEMISTRY
A EUROPEAN JOURNAL

DOI: 10.1002/chem.200601896

A Conceptual DFT Approach for the Evaluation and Interpretation of Redox Potentials

Jan Moens, Paul Geerlings,* and Goedele Roos[a]

Abstract: Conceptual DFT aims at describing the properties of molecules in interactions by using chemical reactivity descriptors. Herein, the redox behaviour of a given species, as quantified by the redox potential, is linked to DFT-based descriptors. We made use of a hierarchical decomposition of the corresponding half-reactions into one-electron reduction, protonation, dissociation and water-forming or dissociation reactions. Most of these reactions can be readily described through reactivity descriptors, such as the electrophilicity, nucleofugality and electrofugality, as defined in conceptual DFT. The final expression linking the corresponding free energy changes to the redox potential seems to give correct predictions for the redox potentials of bromo, chloro and nitro oxo acids in the gas phase, as in a polarised continuum model.

Keywords: density functional calculations · electrophilicity · nucleofugality · oxo acids · redox chemistry

Introduction

Computational chemistry has evolved to the point that it is sometimes competitive to experiment to obtain precise values for certain molecular properties. Density functional theory (DFT)[1] has played a predominant role in this evolution in the last decade.[2,3] Moreover, by giving precision to widespread but often rather vaguely defined concepts, such as electronegativity, hardness and softness, it affords a non-empirical, numerical evaluation of these concepts. This conceptual DFT branch, as termed by its protagonist Parr,[4] provoked an avalanche of papers[5,6] in which these concepts were used both qualitatively and quantitatively for a variety of molecular properties. Applications to "chemical reactivity" have played a key role in this field since the 1980s and early 1990s, and great interest was paid (also by our group) to a variety of classical organic reactions (electrophilic substitutions,[7] nucleophilic additions,[8] concerted reactions,[9] radical reactions,[10] and acid–base reactions[11]; for a review, see references [5,12]). The study of redox reactions, which often involve complex reaction mechanisms, fell until recently out of the scope of conceptual DFT. Nonetheless, reactions in which electrons are consumed are clean examples of the change in energy of an atom or molecule with the number of electrons. This is one of the key relations on which reactivity indices are based in the framework of conceptual DFT.[13] It is, therefore, surprising that the study of these reactions is still an underdeveloped field. The central problem in the description of electrochemical reactions is that most of these processes take place on the surface of the electrodes. Modelling these types of reactions through quantum chemical means should include diffusion and adsorption processes at the electrode surface, although this model can be simplified if we limit the study to reactions in solution. As a consequence, the electrodes accomplish the role of catalytic surfaces. Their effect will be merely of a kinetic instead of thermodynamic nature. Hence, the calculation of the redox potential will not depend on the nature of the electrodes, which can be replaced by a fictitious electron reservoir. In this study, we approximated this reservoir through an ideal sea of electrons with zero chemical potential. As a result, the reservoir behaves as a perfect electron donor. In recent years it has been shown that accurate calculations of redox potentials are possible by using ab initio methods.[14–20] The aim of the present article is not so much another accurate calculation of redox potentials, but the introduction of a methodology based on descriptors from conceptual DFT, which affords a chemical understanding of the energetics of the redox process. We propose a strategy which makes it possible to link conceptual DFT and computational electrochemistry with the aid of a theoretical de-

[a] J. Moens, Prof. Dr. P. Geerlings, G. Roos
Eenheid Algemene Chemie, Faculteit Wetenschappen
Vrije Universiteit Brussel (VUB)
Pleinlaan 2, Brussels (Belgium)
Fax: (+32) 2-629-3317
E-mail: pgeerlin@vub.ac.be

composition scheme constructed from recurrent steps, such as one-electron reduction reactions, protonation reactions and dissociation reactions. Central in this approach is the idea of writing a thermodynamic property, such as the redox potential, as a sum of reactivity descriptors from conceptual DFT. The value of each descriptor will then measure the propensity of a certain chemical process to take place. We should, however, emphasise that this reaction scheme is not based on any kind of kinetic analysis. In our approach, we focused on the properties of single molecules involved in reduction half-reactions, and tried to define a theoretical descriptor for describing electron uptake by the recipient. Reactions in which charge transfer takes place will be described here through the use of a complete set of reactivity descriptors, namely the electrophilicity,[21,22] nucleofugality[23] and electrofugality,[23] as recently introduced in the context of conceptual DFT.[4] Each reactivity index is capable of measuring the susceptibility of a molecule or molecular fragment to a certain chemical process. Central in this study is the use of electrophilicity to quantify the energy change by electron uptake. This descriptor will act as an approximation of the adiabatic electron affinity, which gives an exact description of one-electron reduction reactions. The nucleofugality and electrofugality will figure here as measures of the leaving-group capacity of the nucleofuges and the electrofuges. Although the term nucleofugality has been known for several decades,[24] it is only recently that Ayers et al. have proposed a rigorous theoretical foundation and an elegant working equation the use of which has also been advocated by the present authors.[25] In this context, the term electrofugality arose in a natural way from the definitions of electrophilicity and nucleofugality.

Redox reactions include a vast class of reaction types, varying from simple cases in which the composition of reactant and product remains the same to complex reactions in which the composition changes drastically. Here, we concentrate on reduction reactions of the oxo acids, such as chloro, nitro and bromo oxo acids. These species form a coherent group with molecules that have a certain analogy in the form of their redox reactions and for which electrochemical properties are well described on an experimental basis.[26] The nitro oxo acids, however, do not behave identically to the chloro and bromo oxo acids, and can therefore be used to test the transferability of the applied method.

Electrochemical reactions are highly dependent on the environment. It is therefore extremely important to take the solvent adequately into account. Several different approaches have already been studied to deal with solvation effects, such as molecular simulations,[27] Langevin dipole moments,[28] integral equation techniques[29] and dielectric continuum methods.[30–32] The dielectric continuum method is, in regard to the other methods, broadly applicable and capable of calculating the solvation energy with high accuracy.[31] Herein, we therefore used such an approach with the polarised continuum model (PCM) as a dielectric continuum method.[33]

Theoretical Background

Conceptual DFT provides sharp definitions of a number of reactivity descriptors for atomic and molecular systems, thus helping us to gain insight into the chemical properties of these systems. Here, the electrophilicity, nucleofugality and electrofugality will be used as reactivity indices for the description of the electrochemical process.

Electrophilicity: A thermodynamic interpretation of the electrophilicity has been given by Parr et al. as a validation of the qualitative suggestion made by Maynard et al.[34] The electrophilicity is a measure of the ability of a molecule to accept electrons from a perfect electron donor (that is, a sea of electrons of zero chemical potential and zero hardness at zero temperature). On the basis of a second-order model for the variation of the energy versus the change in the number of electrons ΔN with constant external potential $\nu(\mathbf{r})$ (that is, the potential due to the nuclei) the energy change is as follows:

$$\Delta E = \mu\Delta N + {}^1\!/_2\eta(\Delta N)^2 \tag{1}$$

with μ, the chemical potential, and η, the chemical hardness, defined by $\mu = (\partial E/\partial N)_\nu$ and $\eta = (\partial E^2/\partial N^2)_\nu$. The system will become saturated with electrons when $\Delta E/\Delta N$ equals zero. Equation (1) reduces to $\Delta E = -\frac{\mu^2}{2\eta}$, in which the corresponding gain in energy has been identified as the electrophilicity, ω, of the system:

$$\omega = \frac{\mu^2}{2\eta} \tag{2}$$

In a finite difference approximation, yielding μ to $-\left(\frac{I+A}{2}\right)$ and η to $I-A$,[3] one obtains:

$$\omega = \frac{(I+A)^2}{8(I-A)} \tag{3}$$

wherein I and A are the ionisation potential and the electron affinity, respectively.

The electrophilicity encloses on the one hand, the tendency of electrons to escape the equilibrium system with a factor μ^2, while the chemical hardness can be seen as the resistance to electron transfer. As shown in Equation (3), the electrophilicity and electron affinity are correlated but not equal. While the electron affinity quantifies the energy change due to the uptake of a single electron, ω is associated with the energy lowering for maximal electron flow.

Nucleofugality and electrofugality: The quality of a leaving group can be quantified through the use of the nucleofugality and electrofugality concepts. A group will act as a good nucleofuge when it readily accepts an entire electron from a system. As compared to the electrophilicity, the nucleofuge is forced to accept an entire electron upon dissociation,

while an electrophile just has to accept a "piece" of an electron from the reservoir.[35] Therefore, the nucleofugality can be seen as a sort of activation energy that has to be overcome upon dissociation. Here, we used the definitions of electrofugality and nucleofugality as proposed by Ayers et al.[23] They considered these indices as fundamental properties of the leaving group, thereby ignoring the complications associated with intermolecular and intramolecular interactions.[36,37] The nucleofugality is defined as a measure of the relative stability of an electron acceptor of charge $q-1$ in comparison with the acceptor fragment with charge $q+\Delta q_{ideal}$ in the presence of a perfect electron donor. The expression for this energy change is:

$$\Delta E_{nucleofuge} = E(q-1) - E(q+\Delta q_{ideal}) = -A + \omega(q) = \frac{(I-3A)^2}{8(I-A)} \tag{4}$$

Similarly, the electrofugality is a measure of the relative stability of an electron donor with charge $q+1$ in comparison with the donor fragment of charge $q+\Delta q_{ideal}$ in the presence of a perfect electron donor:

$$\Delta E_{electrofuge} = E(q+1) - E(q+\Delta q_{ideal}) = 1 + \omega(q) = \frac{(3I-A)^2}{8(I-A)} \tag{5}$$

expressed in terms of ionisation potential and electron affinity of the electrofugal or nucleofugal fragment.

Redox potentials: The most appropriate way of calculating the redox potential is by using a thermodynamic cycle linking the process in the gas phase with that in solvent.[14–20] The calculation of the Gibbs free energy is summarised in Equations (6) and (7) which show the thermodynamic cycles for the redox potential of oxo acids in the case of an acid [Eq. (6)] and basic [Eq. (7)] environment, respectively.

$$\begin{array}{ccc} X(g) + aH^+(g) + be^-(g) & \rightarrow & Y(g) + cH_2O(g) \qquad \Delta G^\circ_{gas} \\ \uparrow -\Delta G^\circ_{solv} & & \downarrow \Delta G^\circ_{solv} \\ X(aq) + aH^+(aq) + be^-(aq) & \rightarrow & Y(aq) + cH_2O(aq) \qquad \Delta G^\circ_{redox,aq} \end{array} \tag{6}$$

with

$$\Delta G^\circ_{gas} = \Delta G^\circ_{gas}(Y) + c\Delta G^\circ_{gas}(H_2O) - \Delta G^\circ_{gas}(X) - a\Delta G^\circ_{gas}(H^+)$$

and

$$\begin{aligned} \Delta G^\circ_{redox,aq} &= \Delta G^\circ_{aq}(Y) + c\Delta G^\circ_{aq}(H_2O) - \Delta G^\circ_{aq}(X) - a\Delta G^\circ_{aq}(H^+) \\ &= \left(\Delta G^\circ_{gas}(Y) + \Delta G^\circ_{solv}(Y)\right) + c\left(\Delta G^\circ_{gas}(H_2O) + \Delta G^\circ_{solv}(H_2O)\right) \\ &\quad - \left(\Delta G^\circ_{gas}(Y) + \Delta G^\circ_{solv}(X)\right) - a\left(\Delta G^\circ_{gas}(H^+) + \Delta G^\circ_{solv}(H^+)\right) \\ &= \Delta G^\circ_{gas} + \left(\Delta G^\circ_{solv}(Y) + c\Delta G^\circ_{solv}(H_2O) - \Delta G^\circ_{solv}(X) - a\Delta G^\circ_{solv}(H^+)\right) \end{aligned}$$

ΔG°_{gas} is the Gibbs free energy in the gas phase, ΔG°_{aq} is the Gibbs free energy in the aqueous phase and ΔG°_{solv} is the solvation Gibbs free energy. The standard Gibbs free energy of each state in the gas phase is obtained by using Equation (8):

$$\begin{array}{ccc} X(g) + aH_2O(g) + be^-(g) & \rightarrow & Y(g) + cOH^-(g) \qquad \Delta G^\circ_{gas} \\ \uparrow -\Delta G^\circ_{solv} & & \downarrow \Delta G^\circ_{solv} \\ X(aq) + aH_2O(aq) + be^-(aq) & \rightarrow & Y(aq) + cOH^-(aq) \qquad \Delta G^\circ_{redox,aq} \end{array}$$

with

$$\Delta G^\circ_{gas} = \Delta G^\circ_{gas}(Y) + c\Delta G^\circ_{gas}(OH^-) - \Delta G^\circ_{gas}(X) - a\Delta G^\circ_{gas}(H_2O) \tag{7}$$

and

$$\begin{aligned} \Delta G^\circ_{redox,aq} &= \Delta G^\circ_{aq}(Y) + c\Delta G^\circ_{aq}(OH^-) - \Delta G^\circ_{aq}(X) - a\Delta G^\circ_{aq}(H_2O) \\ &= \left(\Delta G^\circ_{gas}(Y) + \Delta G^\circ_{solv}(Y)\right) + c\left(\Delta G^\circ_{gas}(OH^-) + \Delta G^\circ_{solv}(OH^-)\right) \\ &\quad - \left(\Delta G^\circ_{gas}(Y) + \Delta G^\circ_{solv}(X)\right) - a\left(\Delta G^\circ_{gas}(H_2O) + \Delta G^\circ_{solv}(H_2O)\right) \\ &= \Delta G^\circ_{gas} + \left(\Delta G^\circ_{solv}(Y) + c\Delta G^\circ_{solv}(OH^-) - \Delta G^\circ_{solv}(X) - a\Delta G^\circ_{solv}(H_2O)\right) \end{aligned}$$

$$\Delta G^\circ_{gas} = E_{0\,K} + ZPE + \Delta\Delta G_{0\rightarrow 298\,K} \tag{8}$$

The energy at 0 K (E_0) is calculated by using DFT at the optimum geometry. Zero-point energies (ZPEs; unscaled) and thermal contributions ($\Delta\Delta G_{0\rightarrow 298\,K}$) together with entropies have been used to convert internal energies to Gibbs free energies at 298.15 K.[38] Hereby, we assume that reacting species behave as ideal gases within the rigid rotator–harmonic oscillator approximation. In Equation (8), an extra term should be introduced to convert the ΔG°_{gas} state from 1 atm to 1 M:

$$\Delta G^\circ_{gas}(1\,M) = \Delta G^\circ_{gas}\ (1\ atm) + RT\ln(24.46) \tag{9}$$

The connection between the gas and aqueous phases is made through the calculation of the solvation Gibbs free energy of the specific species. In this study, we used a polarised continuum approach (PCM-UAHF; UAHF: united atom Hartree–Fock) to describe the solvent and the interactions with the solute. The ΔG°_{solv} values were computed from Equation (10):

$$\Delta G^\circ_{solv} = G^\circ_{aq} - G^\circ_{gas} \tag{10}$$

in which G°_{aq} is the total Gibbs free energy of the system in solution and G°_{gas} is the equivalent quantity in a vacuum. To take into account small changes in geometry when going from gas to solvent, we reoptimised the geometry of the molecule in PCM.

Through the calculation of the Gibbs free-energy change of the complete reaction, the standard redox potential can be determined through the Nernst equation [Eq. (11)]:

$$E^\circ = -\frac{\Delta G^\circ_{redox,aq}}{nF} \tag{11}$$

in which n is the number of exchanged electrons and F the Faraday constant. The calculated value of $E°$ is thereby relative to the reduction potential of a reference electrode. Here we will use the normal hydrogen electrode (NHE):

$$H^+(aq) + e^- \rightarrow {}^1/_2H_2(g) \quad (12)$$

with an associated free energy change of −4.44 eV.[39]

Methodology

Studied redox reactions: A survey of the redox reactions used in this study can be found in Table 1.[26,40] Central to the idea of this article is the possibility of dividing a global reduction reaction in a couple of recurrent steps. These steps will be described energetically and for some of them we will use reactivity descriptors from conceptual DFT. It seems at first sight that this reaction path is chosen arbitrarily. Nevertheless, we will show that this strategy could be used in each reaction and is also chemically justified. In the following paragraphs, our approach will be elucidated and the necessary reaction steps will be introduced.

Decomposition scheme: The global reaction will be divided into one-electron reduction reactions, protonation reactions, dissociation reactions and the formation or dissociation of water. Concerning the one-electron reduction reactions, the chemical composition of reagent and product remains the same during this reduction. As mentioned in the Introduction, the electrophilicity will be used as an approximation to the adiabatic electron affinity. In comparison with the electron affinity, the electrophilicity has major advantages for the description of electron uptake. First of all, the possibility of making this descriptor local (through the Fukui function[41–43]) offers the opportunity to look at the position in the molecule, which is reduced. Secondly, this descriptor contains extra information about the system's polarisability, which is intimately related to its chemical softness. Thirdly, it conceals inherently the system's electron affinity through the presence of the chemical potential in its definition. The contribution to the reaction Gibbs free energy could then be written as:

$$\Delta G^\circ \propto -\omega \quad (13)$$

An electron uptake will be energetically more favourable when the system possesses a higher electrophilicity. Neglecting the contribution of the entropy change during reaction, Equation (13) could be rewritten as an equality:

$$\Delta G^\circ = -\alpha\omega \quad (14)$$

by introducing a proportionally constant α, which will be considered as a parameter in this work.

Following the one-electron reduction reactions, the protonation reaction will be interpreted as the inverse of an acid dissociation reaction. The energy change of this reaction can be described through the pK_a of the conjugated acid:

$$\Delta G^\circ = -RT\ln\left(\frac{1}{K_a}\right) \quad (15a)$$

$$\Delta G^\circ = RT\ln(K_a) \text{ and } \Delta G^\circ = -2.303\,RT\,pK_a \quad (15b)$$

The pK_a calculation is a troublesome and highly demanding computational burden and, therefore, we chose to calculate the proton affinity and calibrate it to known experimental pK_a values. This method produces Gibbs free energy changes that are of the correct order in size and gives the correct trends in pK_a values of the oxo acids.

For the dissociation step, the following reaction can be taken as an example:

$$HClO_2^- \rightarrow ClO + OH^- \quad (16)$$

Table 1. Survey of the studied reduction reactions of chloro, nitro and bromo oxo acids with their corresponding experimental redox potentials.

Chloro oxo acids	Exptl $E°$ [V]	Bromo oxo acids	Exptl $E°$ [V]
acidic environment		basic environment	
1) $ClO_3^- + 3H^+ + 2e^- \rightarrow HClO_2 + H_2O$	1.214	10) $BrO_3^- + 3H_2O + 6e^- \rightarrow Br^- + 6OH^-$	0.61
2) $HClO_2 + 2H^+ + 2e^- \rightarrow HClO + H_2O$	1.645	11) $BrO_3^- + 2H_2O + 4e^- \rightarrow BrO^- + 4OH^-$	0.492
3) $HClO + H^+ + 2e^- \rightarrow Cl^- + H_2O$	1.482	12) $BrO^- + H_2O + 2e^- \rightarrow Br^- + 2OH^-$	0.761
Chloro oxo acids		Nitro oxo acids	
basic environment		acidic environment	
4) $ClO_2^- + H_2O + 2e^- \rightarrow ClO^- + 2OH^-$	0.66	13) $NO_3^- + 4H^+ + 3e^- \rightarrow NO + 2H_2O$	0.957
5) $ClO^- + H_2O + 2e^- \rightarrow Cl^- + 2OH^-$	0.81	14) $HNO_2 + H^+ + e^- \rightarrow NO + H_2O$	0.983
6) $ClO_3^- + H_2O + 2e^- \rightarrow ClO_2^- + 2OH^-$	0.33	15) $NO_3^- + 3H^+ + 2e^- \rightarrow HNO_2 + H_2O$	0.934
Bromo oxo acids		Nitro oxo acids	
acidic environment		basic environment	
7) $HBrO + H^+ + 2e^- \rightarrow Br^- + H_2O$	1.331	16) $NO_3^- + H_2O + 2e^- \rightarrow NO_2^- + 2OH^-$	0.01
8) $BrO_3^- + 6H^+ + 6e^- \rightarrow Br^- + 3H_2O$	1.423	17) $NO_2^- + H_2O + e^- \rightarrow NO + 2OH^-$	−0.46
9) $BrO_3^- + 5H^+ + 4e^- \rightarrow HBrO + 2H_2O$	1.447		

The energy change during this reaction is described through the electrofugality and nucleofugality. Here, the nucleofugality of the leaving group, OH^-, and the electrofugality of ClO have to be calculated. These descriptors both relate to the thermodynamic stability of the nucleofuge/electrofuge, and thus the contribution to the Gibbs free energy is described as follows:

$$\Delta G^\circ = \beta(\Delta E_{\text{electrofuge}} + \Delta E_{\text{nucleofuge}}) \tag{17}$$

This equation introduces a proportionally constant β that will be considered as a parameter in this work.[44] Throughout, OH^- will systematically be used as a leaving group in the dissociation reaction. A point of criticism would be that OH^- is not an appropriate leaving group and therefore other groups, such as H_2O, should be considered. Let us underline that the nucleofugality of OH^- is merely used as a constant-energy contribution throughout the different reactions. If H_2O was used as the leaving group instead of OH^-, the electrofuge would remain the same and as a consequence also its electrofugality. As a result, Equation (17) would only change with a constant term.

The last reaction step that has to be introduced into the reaction scheme is the formation or dissociation of water. In an acid environment, dissociation reactions producing OH^- ions would result in a net production of OH^- ions. To prevent this net production, reactions wherein water is formed needed to be included in the global decomposition scheme. In a basic environment, a net consumption of H^+ will take place; therefore, an extra dissociation of water has to be included. The contribution to the Gibbs free energy is then $\Delta G^\circ = -RT\ln(K_W/55.56)$ when water dissociates and $\Delta G^\circ = -RT\ln(55.56/K_W)$ when water is produced, with K_W equal to 1.00×10^{-14} at 298.15 K.

The total energy change on the basis of these different reaction steps becomes:

$$\Delta G^\circ = -\alpha \sum_i^{\text{red.}} \omega_i - 2.303RT \sum_i^{\text{prot.}} \text{p}K_{ai} + \beta \sum_i^{\text{diss.}} \Delta E_{\text{leaving},i} - j(RT\ln(K')) \tag{18}$$

in which the summation runs over the number of reduction, protonation and dissociation reactions, respectively. The factor j equals the number of water dissociation or formation reactions in the reaction scheme. In this equation α and β are two parameters and K' is equal to $K_W/55.56$ when water is dissociated or $55.56/K_W$ when water is formed. The standard redox potential then becomes:

$$E^\circ = \frac{1}{nF}\left(\alpha \sum_i \omega_i + 2.303RT \sum_i \text{p}K_{ai} - \beta\Delta E_{\text{leaving}} + RT\ln(K')\right) \tag{19}$$

On the basis of the foregoing discussion of the various reaction steps, it must be clear that this scheme leaves many ways open for writing a reaction scheme of a reduction reaction. However, a number of considerations based on chemical intuition significantly reduce the possibilities and leave just one possibility open to use as reaction scheme. In order to propose a design for a reaction scheme that can be used in each redox reaction, the identification of the types of starting products is important. As can be seen from Table 1, anions and neutral molecules are starting products from which further reaction takes place. Defining rules for these species will consequently lead to rules for cations.

Anions, cations and neutral molecules: The basic reactions for anions, cations and neutral molecules in the reaction scheme considered are proposed and analysed. An anion is considered to dissociate with the formation of an OH^- group and a corresponding electrofuge if it possesses a proton. Otherwise, the formation of OH^- as leaving group is impossible. We consider protonation reactions of an anion when it does not already possess a proton. Although this principle seems weak at first sight, it will result in a significant simplification of the problem. Protonation reactions could find place on different positions in the molecule (such as on an OH group or an oxygen atom). Taking these possibilities into account will only result in a more complex problem. Reduction reactions for anions are not considered because it will force a negative system to accept another electron.

For neutral molecules neither protonation nor dissociation reactions are considered. A dissociation reaction will result in a positive electrofuge, which may cause problems when forming reagents such as Cl^+. These reactions form products which are chemically improbable. A protonation reaction will result in a positively charged molecule. As a consequence, subsequent reactions must be a reduction or dissociation reaction. However, in the case of H_2ClO^+ this would lead to dissociation reactions for which the only possible leaving group will be water. We wanted to preserve OH^- as a transferable leaving group over the different reaction schemes, and therefore the protonation of neutral molecules is not considered. Reduction reactions are the only reactions examined for neutral molecules.

As a consequence of the previous discussion about anions and neutral molecules, it is impossible to generate positively charged molecules. Therefore, no rules have to be set for cations. These basic principles are summarised in Table 2. Taking these principles into account, one possible reaction scheme remains which can be used in each reaction of the studied oxo acids. The resulting scheme for the case of the reduction of chlorite in acid and basic environments is given in Table 3.

It is, however, possible to construct new pathways if other choices are made in Table 2. As the Gibbs free energy is a state function, one is free to select the reaction path. Consider, for example, a protonation step for neutral molecules; this will lead to the formation of species such as $R{-}H_2O^+$. These structures turned out to give computational problems during optimisation and therefore were not used to build up

Table 2. Summary of the different reaction types considered for anions, cations and neutral molecules. An "A" corresponds to an accepted process while "NA" is used for a process which is systematically rejected.

	Anion	Neutral molecule	Cation
Electron uptake	NA	A	NA
Dissociation reaction	A	NA	NA
Protonation reaction	A	NA	NA

Table 3. Two examples of the decomposition scheme for chlorite in acidic and basic environments.

Acidic environment	Basic environment
$HClO_2+2H^++2e^-\rightarrow HClO+H_2O$	$ClO_2^-+H_2O+2e^-\rightarrow ClO^-+2OH^-$
$HClO_2+e^-\rightarrow HClO_2^-$	$H_2O\rightarrow H^++OH^-$
$HClO_2^-\rightarrow ClO+OH^-$	$ClO_2^-+H^+\rightarrow HClO_2$
$ClO+e^-\rightarrow ClO^-$	$HClO_2+e^-\rightarrow HClO_2^-$
$ClO^-+H^+\rightarrow HClO$	$HClO_2^-\rightarrow ClO+OH^-$
$OH^-+H^+\rightarrow H_2O$	$ClO+e^-\rightarrow ClO^-$

the reaction scheme. From the previous discussion the proposed reaction scheme is proven to be chemically sound and computationally convenient.

Computational details: All calculations were performed by using the Gaussian 03 software.[45] Geometry optimisations were performed at the 6-311++G(d,p) level by using the B3LYP functional.[46] Frequency calculations were used to verify that the structure lies in a minimum of the potential energy surface. Electrophilicity, nucleofugality and electrofugality were calculated by using vertical ionisation potentials and electron affinities. The solvent was taken into account by using a PCM model. Specifically, we used a polarised continuum model (PCM-UAHF)[33] wherein the shape of the dielectric cavity is built up by putting a sphere around each heavy atom. Hydrogen atoms are enclosed in the sphere of the atom to which they are bonded. Structures were always reoptimised in solvent.

Results and Discussion

Thermodynamic cycle: One way to calculate the redox potential of reduction reactions is by using a thermodynamic cycle, such as those presented in Equations (6) and (7). With the aid of these schemes for an acid or basic environment, respectively, redox potentials were calculated relative to the NHE. Table 4 gives an overview of the results.

A high correlation coefficient (0.95; see Figure 1) was found between the experimentally and theoretically calculated redox potentials, with an average discrepancy of 0.13 V. The calculation of the redox potential is highly sensitive to perturbations in the Gibbs free energy. As 1 kcal mol^{-1} corresponds to a redox potential change of 0.043 V, an error of 0.13 V corresponds to 3.0 kcal mol^{-1}. The source of this error should be found in the incompleteness of the description of the solvent. Improvements in solvation models will therefore result in more accurate calculations of redox potential.

Table 4. Survey of calculated redox potentials (column 3) by using Equations (6) and (7) and calculated redox potentials by using Equation (19) in the gas phase (column 4) and in solvent (column 5) versus experimental values (column 2). Calculations are made at the 6-311++G(d,p) level by using the B3LYP functional.

No.[a]	$E°$(exptl) [V]	$E°$ (calcd) [V]	$E°$ (calcd, gas) [V]	$E°$ (calcd, solvent) [V]
1	1.214	1.716	1.215	1.215
2	1.645	2.055	1.400	1.368
3	1.482	1.538	1.325	1.573
4	0.66	0.851	0.319	0.317
5	0.81	1.055	0.627	0.852
6	0.33	0.571	0.200	0.191
7	1.331	1.339	1.335	1.645
8	1.423	1.647	1.344	1.481
9	1.447	1.780	1.348	1.400
10	0.61	0.703	0.412	0.550
11	0.492	0.414	0.300	0.343
12	0.761	0.943	0.636	0.963
13	0.957	0.957	1.176	1.101
14	0.983	0.890	1.405	1.190
15	0.934	0.949	1.061	1.057
16	0.01	−0.176	0.040	0.042
17	−0.46	−0.635	−0.279	−0.506
rms[b]		0.13	0.20	0.17
R^2[c]		0.95	0.88	0.92

[a] See Table 1 for list of studied reactions. [b] Root-mean-square errors. [c] Correlation coefficient (R^2 value).

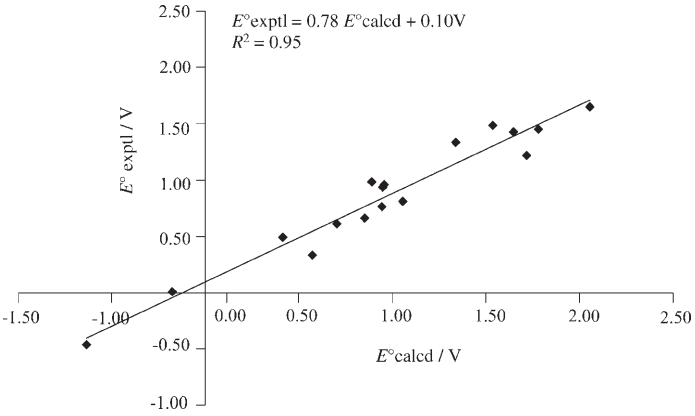

Figure 1. Correlation between the calculated redox potential and experimental values through a thermodynamic cycle for chloro, bromo and nitro oxo acids.

The conceptual DFT approach: As mentioned above, a conceptual DFT-based expression for the redox potential is proposed involving a few approximations. In order to verify this formula, it is necessary to check the correctness of our approximations. Firstly, the electrophilicity is used instead of the electron affinity. Figure 2 shows the relationship between A and ω in the gas phase and in solvent. It is clear from Figure 2 that this approximation is justified when noting the high correlation coefficient. Secondly, the protonation step is described by using the proton affinity instead of the pK_a. The proton affinity is a measure of the change in electronic energy between the protonated and unprotonated forms. Linking proton affinity to pK_a values requires a cor-

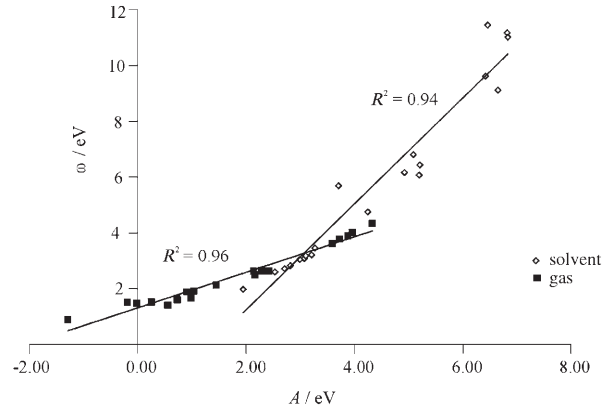

Figure 2. Relationship between the electron affinity (A) and the electrophilicity in the gas phase (■) and in solvent (◇).

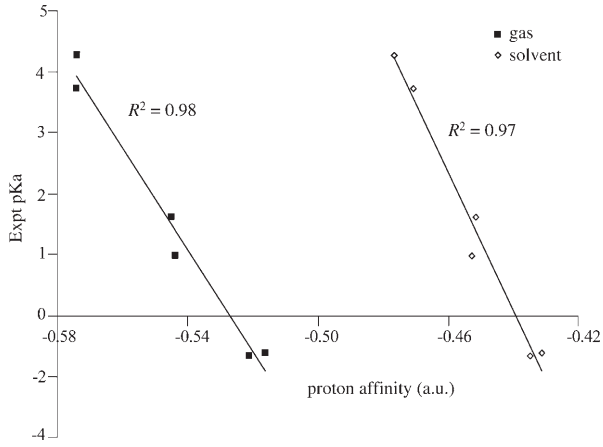

Figure 3. Relationship between the proton affinity (in a.u.) and the pK_a calculated in the gas phase (■) and in solvent (◇). From these calibration curves, pK_a values could be computed from proton affinities.

rect scaling and the introduction of a constant term to take entropic contributions and Gibbs free energies of the proton into account. Therefore, we used a calibration curve between the proton affinity and some experimental values of the pK_A for making subsequent calculations of unknown pK_a values possible. As shown in Figure 3, the high correlation coefficient between proton affinity and pK_a highlights the correctness of this approximation. Thirdly, the dissociation reaction is described by using the electrofugality and nucleofugality. As already discussed, the nucleofugality of OH^- appears as a constant in Equation (19). The electrofugality is used to make a difference in the leaving capacity of the electrofugal fragment. An increase in $\Delta E_{electrofuge}$, which corresponds to a weaker leaving group, seems to be correlated with a weaker base. This is readily understood by considering the follow reaction:

$$ClO_2^- + H^+ \rightarrow HClO_2 \quad (20)$$

This reaction can be seen as an electron-transfer reaction from the electron donor to H^+. A lower value of $\Delta E_{electrofuge}$ is related to a group that more easily donates an electron. This corresponds to a more energetically favourable reaction and therefore to a stronger base (and a higher pK_a value). Striking is that this relationship stands firm between the groups of the chloro and bromo oxo acids in the gas phase, except for the trend between BrO_3^- and ClO_3^- which

Table 5. Overview of values for the electrophilicity (ω), $\Delta E_{electrofuge}$ and $\Delta E_{nucleofuge}$ for the species necessary to compute Equation (19) in the gas phase and solvent. The proton affinity of anions in gas and solvent are expressed in a.u. Experimental pK_a values are given as in reference [40].

	ω [eV]			$\Delta E_{electrofuge}$ [eV]			Proton affinity [a.u.]			Exptl pK_a
	Gas	PCM		Gas	PCM		Gas	PCM		
$HClO_3$	1.881	3.076	ClO_3^-	4.689	8.312	ClO_3^-	−0.516	−0.431	ClO_3^-	−1
$HClO_2$	1.592	3.041	ClO_2^-	2.970	6.753	ClO_2^-	−0.544	−0.453	ClO_2^-	1.98
HClO	1.521	2.819	ClO^-	2.715	7.183	ClO^-	−0.574	−0.471	ClO^-	7.46
$HBrO_3$	1.912	3.212	BrO_3^-	4.770	8.484	BrO_3^-	−0.517	−0.434	BrO^-	8.55
$HBrO_2$	1.668	3.454	BrO_2^-	2.934	7.039	BrO_2^-	−0.546	−0.457	NO_3^-	−1.3
HBrO	1.654	3.172	BrO^-	2.632	7.469	BrO^-	−0.574	−0.477	NO_2^-	3.25
Cl	3.772	11.01	Cl^-	3.902	7.442	NO_3^-	−0.521	−0.435		
Br	3.614	11.44	Br^-	3.684	7.148	NO_2^-	−0.545	−0.451		
HNO_3	1.501	2.597	NO_3^-	4.193	8.258	NO^-	−0.553	−0.449		
HNO_2	1.461	2.714	NO_2^-	3.194	7.257					
HNO	1.403	5.684	NO^-	0.579	6.622					
ClO_2	2.491	6.161								
ClO	2.620	6.064								
BrO_3	4.332	11.16								
BrO_2	2.630	6.802								
BrO	2.641	6.428								
NO_3	4.007	9.107								
NO_2	2.117	4.747								
NO	0.876	1.972								

		$\Delta E_{nucleofuge}$ [eV]	
		Gas	PCM
	OH	0.695	−5.809

is inverted (see Table 5): $\Delta E_{electrofuge}$ $BrO_3^- > ClO_3^- > ClO_2^- > BrO_2^- > ClO^- > BrO^-$; pK_a $BrO^- > ClO^- > BrO_2^- > ClO_2^- > BrO_3^- > ClO_3^-$. Considering the different contributors to the electrofugality in the gas phase, the ionisation potential is much bigger than the electrophilicity. As a consequence, the trend is merely a result of the ionisation potential.

Parameters α and β: The central problem that remains is the presence of two parameters α and β. This issue can be surmounted by using two reference reduction reactions. More concretely, the following reactions will be used [Eq. (21),(22)]:

$$ClO_3^- + 2H^+ + e^- \rightarrow ClO_2 + H_2O \text{ with } E^\circ = 1.152\,V \quad (21)$$

$$ClO_2 + H^+ + e^- \rightarrow HClO_2 \text{ with } E^\circ = 1.277\,V \quad (22)$$

Although every couple of redox reactions can be used, the proposed references are very useful in the calibration of α and β. The second reaction can be used for optimising parameter α, as no dissociation reaction takes place, while the first reaction can be used to calibrate parameter β with the knowledge of α. These parameters are then calculated through the fitting of calculated redox potentials to the experimental values.[40] In the following sections, we will prove that this strategy is capable of reproducing redox potentials not only of chloro oxo acids but also of nitro and bromo oxo acids, indicating that our approach has a transferable character.

Survey of the results: In the gas phase, the optimal values of parameters α and β are 0.45 and 0.14, respectively. With the knowledge of these two parameters, redox potentials can be calculated by using Equation (19). The results of calculated versus experimental redox potentials are summarised in Table 4. In the group of oxo acids, the correlation coefficient between experimental and calculated redox potentials exceeds 0.88 with a root-mean-square (rms) error of 0.20 (see Figure 4). The three groups considered as a whole do not influence the correlation coefficient of each remarkably. The proposed equation is able to resolve the differences between families of molecules and also to distinguish between the individual redox processes. Therefore, these results confirm the validity of Equation (19) and the parameters α and β as universal parameters. Comparing the energy contributions of the different steps, it is clear from Figure 5 that the greatest contributor is without any doubt the electrophilicity. This should not be a surprise, because after all we wanted to describe an electron-uptake process. A higher value of the electrophilicity corresponds to a reagent which is more

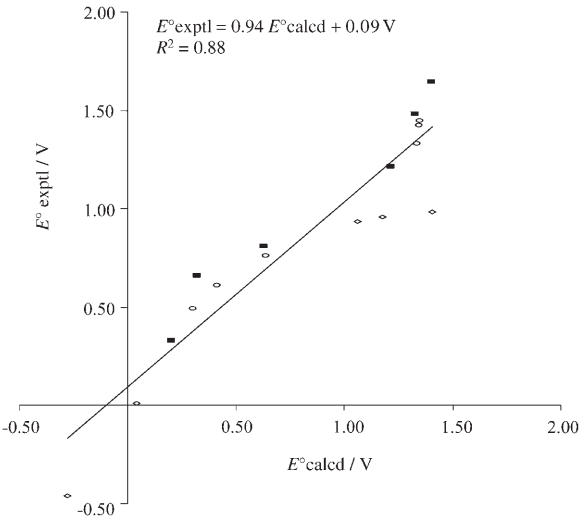

Figure 4. Calculated versus experimental redox potentials by using Equation (19) in the gas phase for chloro (■), nitro (◇) and bromo oxo acids (○).

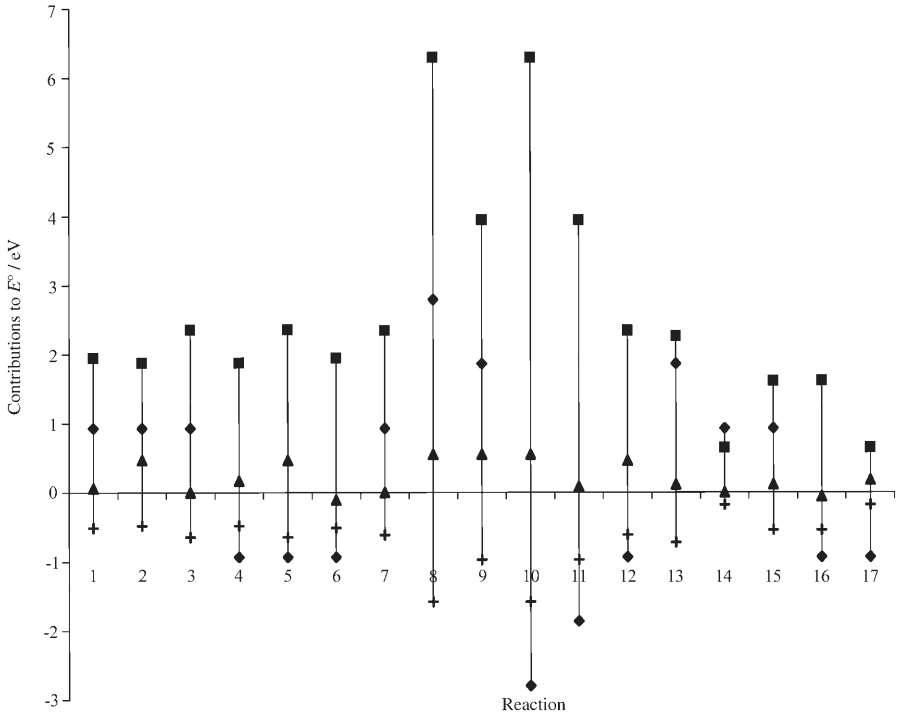

Figure 5. Contributions to the redox potential of the different steps by using scaled electrophilicity and dissociation steps (with parameter values $\alpha = 0.45$ and $\beta = 0.14$) and the sign of the different terms for the different reactions (see Table 1) in the gas phase. ■ = ω (eV, scaled), ▲ = pK_a, ◆ = water and + = dissociation (scaled).

prone to electron uptake. However, Figure 5 also confirms the importance of the other terms in ascertaining good correlations. The nucleofugality and electrofugality express the ease of the dissociation reaction. A lower value of these descriptors is linked to a more favourable dissociation step. The electrophilicity, the nucleofugality and the electrofugality form a complete family of concepts, which makes it possible to derive information about a system's redox potential. Each index is capable of describing the susceptibility of a system for a specific chemical process. Figure 5 shows an explanation of why redox reactions in acid have a higher redox potential than in a basic environment. This is a result of water dissociation reactions, which take place in reaction schemes in a basic environment. These contributions are energetically positive and as a consequence they scale down redox potential values as compared to the same reaction in an acid environment.

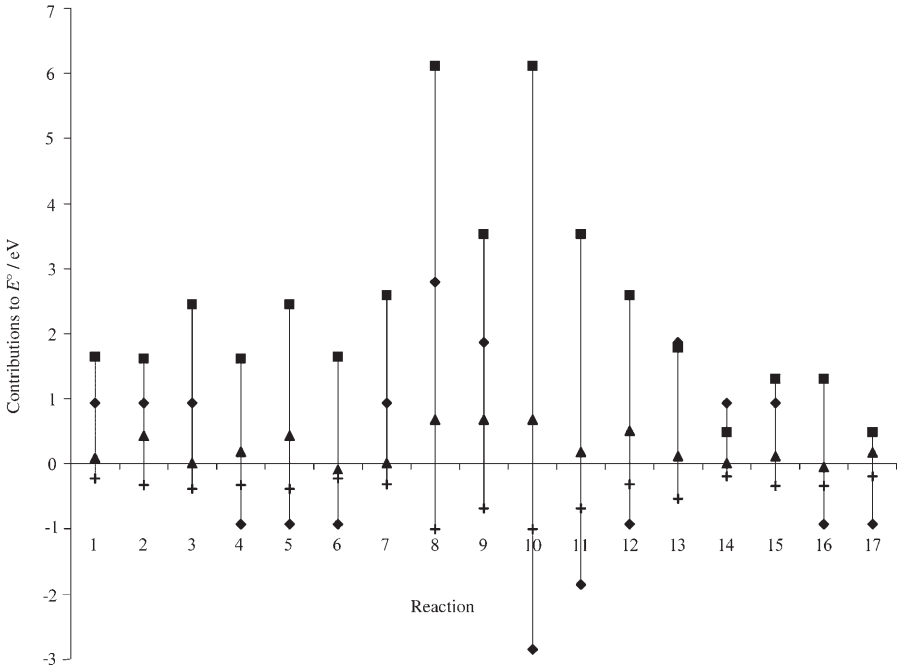

Figure 7. Contributions to the redox potential of the different steps using scaled electrophilicity and dissociation steps (with parameter values $\alpha = 0.18$ and $\beta = 0.24$) and the sign of the different terms for the different reactions (see Table 1) in solvent. ■ = ω (eV, scaled), ▲ = pK_a, ◆ = water and + = dissociation (scaled).

Taking the solvent water into account through a PCM model will have an influence on the values of the electrophilicity, nucleofugality and electrofugality. The reason for this change is the strong stabilisation of charged species in solvent. The values for the ionisation potential are diminished, while the electron affinity increases. Bringing these reagents into solvent makes them softer and more ready for electron uptake. Therefore, the electrophilicity will increase while the nucleofugality decreases. The electrofugality will also increase because the capacity for giving one electron diminishes. As a consequence, the parameters α and β differ from those in the gas phase. The term involving the nucleofugality of OH^- becomes very negative, and therefore contributions of the dissociation reactions are smaller and the coefficient β increases as compared to α ($\alpha = 0.18$ and $\beta = 0.24$). A correct scaling of the electrophilicity and the dissociation step will be insurmountable if redox potentials need to be correctly calculated. Again the excellent correlation coefficient in PCM convinces us of the correctness of the methodology (see Figure 6). The predictive ability of these results is high, as leave-one-out correlation coefficients are not substantially different from the correlation coefficients with the full data set. In the gas phase, maximum decreases in R^2 of 0.03 and in PCM of 0.04 are found. The energetic contribution of the different terms in PCM (Figure 7) is comparable to those in the gas phase. The parameters α and β scale the contributions of the dissociation and reduction reactions, so that in gas and in solvent these values are of comparable size.

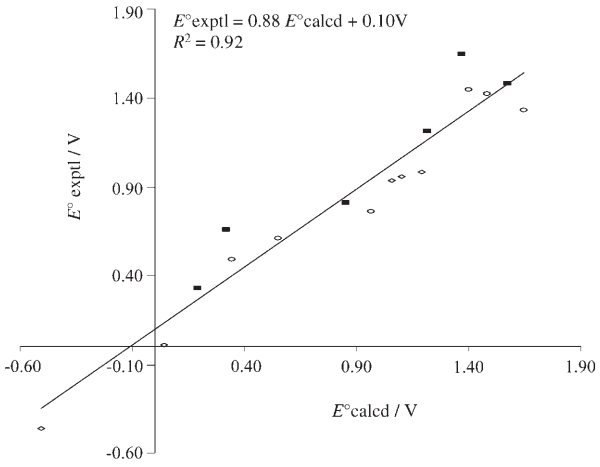

Figure 6. Relation between the calculated redox potential by using Equation (19) and the experimental redox potential in solvent for chloro (■), nitro (◇) and bromo oxo acids (○).

Conclusions

Herein, we have examined the ability of a conceptual DFT-based theoretical approach to calculate redox potentials in the gas and solution phases. Conceptual DFT descriptors are used to describe the important chemical processes involved, such as the electron uptake and dissociation reaction. Our approach to writing the reduction reaction as a

sum of recurrent steps seems to be profitable in a vast class of oxo acids. As compared to methods using thermodynamic cycles, the proposed model offers the opportunity to interpret the chemistry behind redox reactions. We have shown that the largest contributors to the redox potentials are the values of the electrophilicity and the energy change for dissociation or formation of water. Nevertheless, the other terms could not be disregarded in the global picture. A large value of the electrophilicity is linked to a favourable electron-uptake process, while low values of nucleofugality and electrofugality correspond to easy dissociation reactions. This group of indices seems to be complete in the description of the redox process. The final expression contains only two parameters, α and β, which can be readily optimised and were shown to be transferable between the different groups of oxo acids.

In this study, we limited ourselves to the examination of singly charged oxo acids. Future work should confirm the possibility of using the expression for other groups, such as phospho oxo acids, in which doubly and triply charged species occur.

Acknowledgements

P.G. thanks the Fund for Scientific Research Flanders (FWO) and the VUB for continuous support of his research group. J.M. and G.R. thank the Fund for Scientific Research Flanders (FWO) for a predoctoral (Aspirant) fellowship. The authors thank Professor P. W. Ayers (McMaster, Canada) for stimulating discussions in the initial stage of this work.

[1] P. Hohenberg, W. Kohn, *Phys. Rev. B* **1964**, *136*, 864–871.
[2] W. Koch, M. C. Holthausen, *A Chemist's Guide to Density Functional Theory*, Wiley-VCH, Weinheim, **2000**.
[3] R. G. Parr, W. Yang, *Density Functional Theory of Atoms and Molecules*, Oxford University Press, Oxford, **1989**.
[4] R. G. Parr, W. Yang, *Annu. Rev. Phys. Chem.* **1995**, *46*, 701–728.
[5] P. Geerlings, F. De Proft, W. Langenaeker, *Chem. Rev.* **2003**, *103*, 1793–1874.
[6] H. Chermette, *J. Comput. Chem.* **1999**, *20*, 129–154.
[7] W. Langenaeker, K. Demel, P. Geerlings, *J. Mol. Struct. (THEOCHEM)* **1991**, *234*, 329–342.
[8] W. Langenaeker, K. Demel, P. Geerlings, *J. Mol. Struct. (THEOCHEM)* **1992**, *259*, 317–330.
[9] S. Damoun, G. Van de Woude, F. Mendez, P. Geerlings, *J. Phys. Chem. A* **1997**, *101*, 886–893.
[10] A. K. Chandra, M. T. Nguyen, *J. Chem. Soc. Perkin Trans. 2* **1997**, 1415.
[11] F. De Proft, W. Langenaeker, P. Geerlings, *Tetrahedron* **1995**, *51*, 4012–4032.
[12] P. Geerlings, F. De Proft, *Int. J. Quantum Chem.* **2000**, *80*, 227–235.
[13] R. F. Nalewajski, R. G. Parr, *J. Chem. Phys.* **1982**, *77*, 399–407.
[14] K. S. Raymond, A. K. Grafton, R. A. Wheeler, *J. Phys. Chem. B* **1997**, *101*, 623–631.
[15] E. V. Patterson, C. J. Cramer, D. G. Truhlar, *J. Am. Chem. Soc.* **2001**, *123*, 2025–2031.
[16] M.-H. Baik, J. S. Silverman, I. V. Yang, P. A. Ropp, V. A. Szalai, W. Yang, H. H. Thorp, *J. Phys. Chem. B* **2001**, *105*, 6437–6444.
[17] M.-H. Baik, R. A. Friesner, *J. Phys. Chem. A* **2002**, *106*, 7407–7412.
[18] M. Uudsemaa, T. Tamm, *J. Phys. Chem. A* **2003**, *107*, 9997–10003.
[19] M. N. P. Norouzi, R. Ranjbar, *J. Mol. Struct. (THEOCHEM)* **2003**, *625*, 235–241.
[20] Y. Fu, L. Liu, Y.-M Wang, J.-N Li, T.-O. Yu, O.-X Guo, *J. Phys. Chem. A* **2006**, *110*, 5874–5886.
[21] R. G. Parr, L. V. Szentpály, S. Liu, *J. Am. Chem. Soc.* **1999**, *121*, 1922–1924.
[22] P. K. Chattaraj, U. Sarkar, D. R. Roy, *Chem. Rev.* **2006**, *106*, 2065–2091.
[23] P. W. Ayers, J. S. M. Anderson, J. I. Rodriguez, Z. Jawed, *Phys. Chem. Chem. Phys.* **2005**, *7*, 1918–1925.
[24] C. J. M. Stirling, *Acc. Chem. Res.* **1979**, *12*, 198–203.
[25] G. Roos, S. Loverix, S. E. Brosens, K. Van Belle, L. Wyns, P. Geerlings, J. Messens, *ChemBioChem* **2006**, *7*, 981–989.
[26] D. F. Shriver, P. W. Atkins, *Inorganic Chemistry*, 3rd ed., Oxford University Press, Oxford, **1999**.
[27] W. L. Jorgensen, J. M. Briggs, J. Gao, *J. Am. Chem. Soc.* **1987**, *109*, 6857–6858.
[28] J. Florian, A. Warshel, *J. Phys. Chem. B* **1997**, *101*, 5583–5595.
[29] C. Lim, D. Bashford, M. Karplus, *J. Phys. Chem.* **1991**, *95*, 5610–5620.
[30] C. J. Cramer, D. G. Truhlar, *Chem. Rev.* **1999**, *99*, 2161–2200.
[31] J. Tomasi, B. Mennucci, R. Cammi, *Chem. Rev.* **2005**, *105*, 2999–3094.
[32] J. Tomasi, M. Persico, *Chem. Rev.* **1994**, *94*, 2027–2094.
[33] a) R. Cammi, B. Mennucci, J. Tomasi, *J. Phys. Chem. A* **1998**, *102*, 870–875; b) R. Cammi, B. Mennucci, J. Tomasi, *J. Phys. Chem. A* **2000**, *104*, 4690–4698.
[34] A. T. Maynard, M. Huang, W. G. Rice, D. G. Covell, *Proc. Natl. Acad. Sci. USA* **1998**, *95*, 11578–11583.
[35] P. W. Ayers, J. S. M. Anderson, L. J. Bartolotti, *Int. J. Quantum Chem.* **2005**, *101*, 520–534.
[36] P. R. Campodonico, A. Aizman, R. Contreras, *Chem. Phys. Lett.* **2006**, *422*, 340–344.
[37] P. Jaramillo, L. R. Domingo, P. Perez, *Chem. Phys. Lett.* **2006**, *420*, 95–99.
[38] W. J. Hehre, L. Radom, P. v. R. Schleyer, J. A. Pople, *Ab Initio Molecular Orbital Theory*, Wiley, New York, **1986**.
[39] S. Trasatti, *Pure Appl. Chem.* **1986**, *58*, 955–966.
[40] *CRC Handbook of Chemistry and Physics* (Ed.: D. R. Lide), 75th ed., CRC Press, Boca Raton.
[41] P. Pérez, A. Toro-Labbé, A. Aizman, R. Contreras, *J. Org. Chem.* **2002**, *67*, 4747–4752.
[42] E. Chamorro, P. K. Chattaraj, P. Fuentealba, *J. Phys. Chem. A* **2003**, *107*, 7068–7072.
[43] P. K. Chattaraj, B. Maiti, U. Sarkar, *J. Phys. Chem. A* **2003**, *107*, 4973–4975.
[44] This equation is consistent with the proven link between the stability towards heterolytic cleavage and the maximal hardness principle; see, for example: P. K. Chattaraj, A. Cedillo, R. G. Parr, *J. Org. Chem.* **1995**, *60*, 4707–4714.
[45] Gaussian 03 (Revision B.03), M. J. Frisch, G. W. Trucks, H. B. Schlegel, G. E. Scuseria, M. A. Robb, J. R. Cheeseman, J. A. Montgomery, Jr., T. Vreven, K. N. Kudin, J. C. Burant, J. M. Millam, S. S. Iyengar, J. Tomasi, V. Barone, B. Mennucci, M. Cossi, G. Scalmani, N. Rega, G. A. Petersson, H. Nakatsuji, M. Hada, M. Ehara, K. Toyota, R. Fukuda, J. Hasegawa, M. Ishida, T. Nakajima, Y. Honda, O. Kitao, H. Nakai, M. Klene, X. Li, J. E. Knox, H. P. Hratchian, J. B. Cross, C. Adamo, J. Jaramillo, R. Gomperts, R. E. Stratmann, O. Yazyev, J. Austin, R. Cammi, C. Pomelli, J. W. Ochterski, P. Y. Ayala, K. Morokuma, G. A. Voth, P. Salvador, J. J. Dannenberg, V. G. Zakrzewski, S. Dapprich, D. Daniels, M. C. Strain, O. Farkas, D. K. Malick, A. D. Rabuck, K. Raghavachari, B. Foresman, J. V. Ortiz, Q. Cui, A. G. Baboul, S. Clifford, J. Cioslowski, B. B. Stefanov, G. Liu, A. Liashenko, P. Piskorz, I. Komaromi, R. L. Martin, D. J. Fox, T. Keith, M. A. Al-Laham, Y. Peng, A. Nanayakkara, M. Challacombe, P. M. W. Gill, B. Johnson, W. Chen, M. W. Wong, C. Gonzalez, J. A. Pople, Gaussian, Inc., Pittsburgh, PA, **2003**.
[46] a) A. D. Becke, *J. Chem. Phys.* **1993**, *98*, 5648–5652; b) C. Lee, W. Yang, R. G. Parr, *Phys. Rev. B* **1988**, *37*, 785–789.
[47] The hydration Gibbs free energy of the proton ($\Delta G^{\circ}_{solv}(H^{+})$) is not a known experimental quantity. We used a theoretical value of

$-262.23\,\mathrm{kcal\,mol^{-1}}$ as proposed by Tawa et al.[47] For the solvation Gibbs free energy of water ($\Delta G^{\circ}_{solv}(H_2O)$),[40] we used the standard Gibbs free energy of vaporisation at 298.15 K and 1 atm with a concentration of 1 M: $\Delta G^{\circ}_{solv} = -6.3\,\mathrm{kcal\,mol^{-1}}$. The Gibbs free energy of the proton ($G^{\circ}_{gas}(H^+)$) at 1 atm and 298.15 K is determined through the Sackur–Tetrode equation: $G_{gas}(H^+) = -6.28\,\mathrm{kcal\,mol^{-1}}$. G. J. Tawa, I. A. Topol, S. K. Burt, R. A. Caldwell, A. A. Rashin, *J. Chem. Phys.* **1998**, *109*, 4852–4863.

Received: December 22, 2006
Published online: May 15, 2007

